Limnol. Oceanogr., 48(1), 2003, 55–67

Carbon acquisition of bloom-forming marine phytoplankton

Björn Rost,[1] Ulf Riebesell, and Steffen Burkhardt
Alfred Wegener Institute for Polar and Marine Research, P.O. Box 120161, D-27515 Bremerhaven, Germany

Dieter Sültemeyer
Fachbereich Biologie, Universität Kaiserslautern, P.O. Box 3049, D-67653 Kaiserslautern, Germany

Abstract

Carbon acquisition in relation to CO_2 supply was investigated in three marine bloom-forming microalgae, the diatom *Skeletonema costatum*, the flagellate *Phaeocystis globosa*, and the coccolithophorid *Emiliania huxleyi*. In vivo activities of extracellular (eCA) and intracellular (iCA) carbonic anhydrase activity, photosynthetic O_2 evolution, CO_2 and HCO_3^- uptake rates were measured by membrane inlet mass spectrometry in cells acclimated to pCO_2 levels of 36, 180, 360, and 1,800 ppmv. Large differences were obtained between species both with regard to the efficiency and regulation of carbon acquisition. While eCA activity increased with decreasing CO_2 concentration in *S. costatum* and *P. globosa*, consistently low values were obtained for *E. huxleyi*. No clear trends with pCO_2 were observed in iCA activity for any of the species tested. Half saturation concentrations ($K_{1/2}$) for photosynthetic O_2 evolution, which were highest for *E. huxleyi* and lowest for *S. costatum*, generally decreased with decreasing CO_2 concentration. In contrast, $K_{1/2}$ values for *P. globosa* remained unaffected by pCO_2 of the incubation. CO_2 and HCO_3^- were taken up simultaneously by all species. The relative contribution of HCO_3^- to total carbon uptake generally increased with decreasing CO_2, yet strongly differed between species. Whereas $K_{1/2}$ for CO_2 and HCO_3^- uptake was lowest at the lowest pCO_2 for *S. costatum* and *E. huxleyi*, it did not change as a function of pCO_2 in *P. globosa*. The observed taxon-specific differences in CO_2 sensitivity, if representative for the natural environment, suggest that changes in CO_2 availability may influence phytoplankton species succession and distribution. By modifying the relative contribution of different functional groups, e.g., diatomaceous versus calcareous phytoplankton, to the overall primary production this could potentially affect marine biogeochemical cycling and air–sea gas exchange.

Marine phytoplankton account for approximately 50% of global primary production (Falkowski et al. 1998). Changes in the oceanic primary production over geological timescales have influenced biogeochemical cycles and thus atmospheric pCO_2 levels. Of the approximately 20,000 phytoplankton species (Falkowski and Raven 1997), however, only a relatively small number of key species control the cycling of carbon and other bioelements. Among these, bloom-forming phytoplankton play a major role in determining vertical fluxes of particulate material. With respect to their specific effects on biogeochemical cycling, phytoplankton can be separated into so-called functional groups (Falkowski et al. 1998), such as silicifying and calcifying phytoplankton, flagellates, and N_2-fixating cyanobacteria. The relative contribution of each of these groups to marine primary production largely determines biogeochemical cycling in the ocean and the interplay between the various bioelements. What determines the distribution and succession of phytoplankton in space and time, especially with respect to the different functional groups, remains one of the central but still unresolved questions in biological oceanography.

Until recently, the potential role of inorganic carbon acquisition in marine phytoplankton ecology and evolution has largely been ignored, particularly since dissolved inorganic carbon in seawater is always in excess relative to other plant nutrients. The primary carboxylating enzyme, Ribulose-1,5 bisphosphate carboxylase/oxygenase (RubisCO), however, is restricted to CO_2 for carbon fixation. Owing to the low concentrations of aqueous CO_2 present in seawater (5–25 μmol L^{-1}) and the poor substrate affinity of RubisCO for CO_2 (K_M of 20–70 μmol L^{-1}, Badger et al. 1998) photosynthesis of phytoplankton may suffer from CO_2 limitation. To overcome the low CO_2 affinity of their main carboxylating enzyme, most microalgae have developed mechanisms to enhance their intracellular CO_2 concentration relative to external concentrations. These CO_2 concentrating mechanisms (CCMs) comprise active uptake of CO_2 and/or HCO_3^- into the algal cell and/or the chloroplast (e.g., Amoroso et al. 1998). The enzyme carbonic anhydrase (CA), which accelerates the otherwise slow rate of conversion between HCO_3^- and CO_2, is also involved in most CCMs. Significant differences in the catalytic efficiency of RubisCO exist between major algal and cyanobacterial taxa (Badger et al. 1998). These taxonomic differences seem to be reflected in the efficiency of their CCMs, i.e., with decreasing CO_2 affinity of RubisCO the capacity of cells to concentrate inorganic carbon increases (Tortell 2000). Raven (1997) suggested that differences in inorganic carbon acquisition could also impose other resource requirements. After all, differences in the efficiency

[1] Corresponding author (brost@awi-bremerhaven.de).

Acknowledgments

We would like to thank Dr. Gabi Amoroso, Dominik Müller, and Christoph Thyssen for technical support and laboratory assistance and Aaron Kaplan for his constructive comments on the manuscript. This work was supported by the Netherlands-Bremen Cooperation in Oceanography (NEBROC) and by the German–Israeli Cooperation in Marine Sciences (Mars 2/3), which is funded by the German Federal Ministry of Education and Research (BMBF).

and regulation of carbon acquisition between phytoplankton species as well as taxonomic groups may well affect their relative fitness in a resource-limited environment.

In the present study we investigated the changes in carbon acquisition of marine microalgae in response to changes in CO_2 supply. Our test organisms, the diatom *Skeletonema costatum,* the flagellate *Phaeocystis globosa,* and the coccolithophorid *Emiliania huxleyi,* representatives of three phytoplankton functional groups, are all bloom forming and have a worldwide distribution. In each of these species we examined photosynthetic O_2 evolution and quantified CO_2 and HCO_3^- fluxes across the plasmalemma during steady-state photosynthesis by the use of membrane inlet mass spectrometry (Badger et al. 1994). Moreover, activities of extracellular and intracellular CA were determined by monitoring ^{18}O exchange from doubly labeled $^{13}C^{18}O_2$ (Palmqvist et al. 1994). The results of this study are discussed with respect to the considerable variability in CO_2 availability, both on glacial–interglacial time scales and in view of the present rise in atmospheric pCO_2. A better understanding of the mechanisms determining the efficiency and regulation of carbon acquisition may help to improve our ability to predict the responses of marine phytoplankton to future environmental changes.

Material and methods

Culture conditions and sampling—Skeletonema costatum, Phaeocystis globosa (both strains collected in the North Sea and maintained in stock culture for some years), and a calcifying strain of *Emiliania huxleyi* (B92/11) were grown at 15°C in 0.2-μm-filtered and unbuffered seawater (salinity 32), which was enriched with nutrients according to f/2 medium (Guillard and Ryther 1962). Batch cultures were grown in 1-liter glass tubes under continuous light and an incident photon flux density (PFD) of 180 μmol photons m^{-2} s^{-1}. Air containing CO_2 partial pressures (pCO_2) of 36, 180, 360, and 1,800 ppmv was sparged continuously through the cultures, which resulted in a range of pH values between 9.1 and 7.6 (Burkhardt et al. 2001). Prior to mass spectrometric analysis cells were acclimated to the respective conditions for at least 3 d. Cultures in which the pH has shifted significantly in comparison to the cell-free medium at the respective pCO_2 (pH drift > 0.05) were excluded from further analysis.

Prior to the measurements, 800 ml of culture were harvested by centrifugation (500–1,000 $\times$ g, 15°C, 4 min) and the pellet was subsequently washed in CO_2-free f/2 medium, buffered with 2-[4-(2-Hydroxyethyl)-1-piperazinyl]-ethanesulfonic acid (HEPES, 50 mmol L^{-1}, pH 8.0). A subsample of the culture was used for potentiometric pH measurements. Samples for the determination of chlorophyll *a* (Chl *a*) concentration were taken after the measurements by centrifuging 2 ml of the cell suspension (4,500 $\times$ g, 4 min). Chl *a* was subsequently extracted in 1 ml of methanol (1 h in darkness, at 4°C) and determined spectrophotometrically at 652 and 665 nm. Chl *a* concentrations in the cultures ranged from 4 to 35 μg L^{-1} at the time of sampling.

Cell-free samples from each pCO_2 incubation were taken for measurements of dissolved inorganic carbon (Ci) and alkalinity (Alk) in order to determine the carbonate system. Ci and Alk were determined by coulometry (Johnson et al. 1993) and Gran titration (Gran 1952), respectively. The carbonate system was then calculated from Ci, Alk, temperature, salinity, and concentrations of phosphate and silicate using the dissociation constants of Goyet and Poisson (1989).

Determination of CA activity—CA activity was determined from the ^{18}O depletion of doubly labeled $^{13}C^{18}O_2$ in water caused by several hydration and dehydration steps of CO_2 and HCO_3^- (Silverman 1982). This mass spectrometric procedure allows the determination of CA activity from intact cells under conditions similar to those during growth and differentiates between extracellular CA (eCA) and intracellular CA (iCA) activity (Silverman 1982; Burkhardt et al. 2001). All measurements were carried out in an 8-ml thermostated cuvette, which was attached to a quadrupole mass spectrometer (MSD 5970; Hewlett Packard) via a semipermeable membrane inlet system. Changes in the concentrations of the CO_2 isotopes $^{13}C^{18}O^{18}O$ (m/z = 49), $^{13}C^{18}O^{16}O$ (m/z = 47) and $^{13}C^{16}O^{16}O$ (m/z = 45) were recorded continuously and calculated as

$$^{18}O \log(\text{enrichment}) = \log\frac{(^{13}C^{18}O_2) \times 100}{^{13}CO_2} = \log\frac{(49) \times 100}{45 + 47 + 49} \quad (1)$$

Measurements of eCA and iCA activities were performed in CO_2-free f/2 medium buffered with 50 mmol L^{-1} HEPES (pH 8.0) at 15°C. If not stated otherwise, all assays were carried out in the dark. 1 mmol L^{-1} $NaH^{13}C^{18}O_3$ was added and the uncatalyzed rate of ^{18}O loss was recorded for about 8 min followed by the addition of 50–150 μl of the resuspended cells to yield a final Chl *a* concentration of 0.4–3 μg ml^{-1}. Examples for the change in log (enrichment) upon the addition of algal cells to the cuvette in the dark are given in Fig. 1. For calculation of eCA activity, the linear decrease in ^{18}O atom fraction after the addition of the sample (S_2) was compared to the noncatalyzed decline (S_1) and normalized on a Chl *a* basis (Badger and Price 1989):

$$U = \frac{(S_2 - S_1) \times 100}{S_1 \times \text{mg Chl } a} \quad (2)$$

iCA activity was estimated from the rapid decline in log (enrichment) upon the injection of cells and calculated according to Palmqvist et al. (1994). In the latter experiments dextran-bound sulfonamide (DBS; Synthelec AB), an inhibitor of eCA, was added prior to the injection of cells to a final concentration of 100 μmol L^{-1}. In the presence of DBS the final slope equals the initial slope ($S_1 = S_2'$), indicating a complete inhibition of external CA.

Subsequent to the iCA measurements, light was switched on (300 μmol photons m^{-2} s^{-1}) for 3 min. Light-induced changes in the ^{18}O exchange can be indicative for active transport of Ci since there will be an enhanced influx of CO_2 and HCO_3^- into the cell to the active site of iCA, resulting in an increase of the ^{18}O loss (Badger and Price 1989).

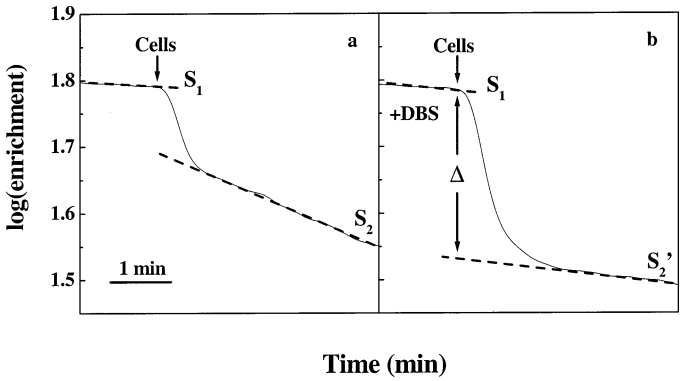

Fig. 1. Changes in the ^{18}O log (enrichment) of doubly labeled $^{13}C^{18}O_2$ for in vivo measurements of (a) eCA and (b) iCA activities. In both experiments the initial linear decline in log(enrichment) (S_1) represents the uncatalyzed rate of ^{18}O exchange. (a) A higher final linear rate of ^{18}O depletion (S_2) is indicative for the presence of eCA activity, which is calculated according to Eq. 2. (b) Intracellular CA activities were determined in the presence of 100 μmol L^{-1} DBS. The drop (Δ) in the log (enrichment) was determined by extrapolating the final slope (S_2') back to the addition of the cells. The data show measurements for *P. globosa* acclimated to 36 ppmv CO_2. For direct comparison the same amount of cells (Chl *a* concentration 0.45 μg ml^{-1}) from the same culture was added in these assays.

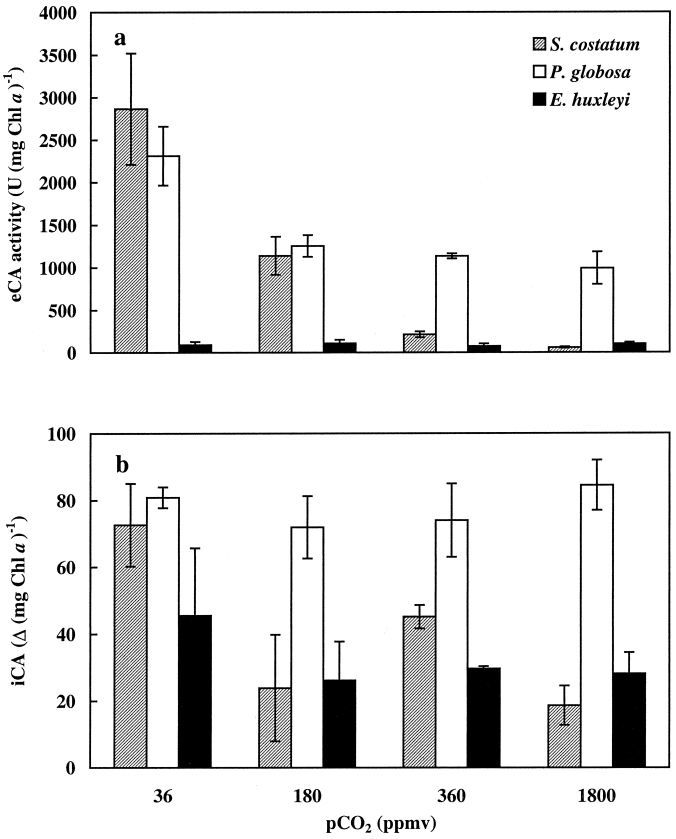

Fig. 2. Chl *a*–specific activities of (a) eCA and (b) iCA for *S. costatum*, *P. globosa*, and *E. huxleyi* as a function of pCO_2 in the culture medium. Values represent the mean of at least three independent measurements (±SD).

Effect of eCA on net photosynthesis—To investigate the potential effect of eCA on net photosynthesis, O_2 evolution was monitored in the absence and presence of DBS (100 μmol L^{-1}). The measurements were performed with cells acclimated to 360 and 180 ppmv CO_2 at concentrations of 3 and 27 μmol CO_2 L^{-1}. The assay conditions were the same as for the carbon flux measurements (*see* below).

Determination of net photosynthesis, CO_2 and HCO_3^- uptake—To investigate inorganic carbon fluxes during steady-state photosynthesis, the same membrane inlet system was used as for the CA measurements. The method established by Badger et al. (1994) is based on simultaneous measurements of O_2 and CO_2 during consecutive light and dark intervals. It has been applied in several studies of cyanobacteria and freshwater microalgae (Palmqvist et al. 1994; Tchernov et al. 1997; Amoroso et al. 1998) and recently also of marine diatoms (Burkhardt et al. 2001).

In the present study we followed largely the protocol described by Burkhardt et al. (2001). All measurements were performed in f/2 medium, buffered with 50 mmol L^{-1} HEPES (pH 8.0) at 15°C. DBS concentration in the cuvette was 100 μmol L^{-1}. Chl *a* concentration ranged between 1 and 3 μg ml^{-1}. Light and dark intervals during the assay lasted 6 and 7 min, respectively. The incident photon flux density was 300 μmol m^{-2} s^{-1}. For further details on the method and calculation we refer to Badger et al. (1994) and Burkhardt et al. (2001).

Results

CA activity—Determination of carbonic anhydrase (CA) activity using membrane inlet mass spectrometry distinguishes between extracellular (eCA) and intracellular (iCA) activity, yet the obtained values are of different denotation. Values for eCA activity are a direct measure for the acceleration in the rate of conversion between CO_2 and HCO_3^- (Fig. 1a) and thus can be used for the comparison of species and different treatments. In *S. costatum*, we observed an almost 60-fold increase in Chl *a*–specific activity of eCA with decreasing CO_2 concentrations (Fig. 2a). The eCA activity in *P. globosa* remained high in all incubations and increased only about twofold from 180 to 36 pCO_2, whereas eCA activity in *E. huxleyi* was low and remained unaffected by pCO_2 in the incubation.

Determination of iCA activity (Δ) in this approach is dependent on the rate of diffusive CO_2 entry into the cell and the rate of intracellular and extracellular ^{18}O depletion (Fig. 1b). Owing to the presence of DBS, the influence of eCA activity was excluded. Factors influencing the diffusive properties of the membranes, such as cell size and shape or intracellular pH potentially affect estimates of iCA activity. Thus Δ values have arbitrary units, which allows the comparison of iCA activities between treatments but not between species. All species tested contained intracellular CA regardless of the growth conditions. The activity of iCA in *P. globosa* and *E. huxleyi* showed no trend with CO_2 in the incubation (Fig. 2b). In contrast, a two to threefold higher

Table 1. Effect of DBS on net photosynthesis expressed as percentage change in the rate upon the addition of 100 μmol L^{-1} DBS. Cells were acclimated to 360 and 180 ppmv CO_2 and tested at CO_2 concentration of 3 and 27 μmol L^{-1} (pH 8.0). Data represent the mean values of three independent measurements (±SD). ND = not determined.

	Effect of DBS on net photosythesis (%)	
pCO_2 (ppmv)	3 μmol L^{-1} CO_2	27 μmol L^{-1} CO_2
S. costatum		
360	−47 ± 6	+4 ± 4
180	−58 ± 12	+2 ± 5
P. globosa		
360	−6 ± 1	+4 ± 4
180	−19 ± 1	+5
E. huxleyi		
360	−1 ± 3	+3 ± 4
180	ND	+1 ± 2

enzyme activity was observed in cells of *S. costatum* grown at 36 pCO_2 compared to cells grown at higher pCO_2 levels.

To test the effect of eCA on photosynthesis in cells acclimated to 180 and 360 ppmv CO_2, we monitored the O_2 evolution prior to and after the addition of DBS (100 μmol L^{-1}) at CO_2 concentrations of 3 and 27 μmol L^{-1}. At the high CO_2 concentration DBS did not inhibit net photosynthesis in any of the investigated species (Table 1; Fig. 3). At the low CO_2 concentration, net photosynthesis of *S. costatum* was inhibited by 47% and 58% in 360 and 180 ppmv acclimated cells, respectively. For *P. globosa* the inhibition of net photosynthesis at the low CO_2 concentration was 6% for 360 ppmv acclimated cells and increased to 19% (180 ppmv acclimated cells). In *E. huxleyi* no inhibition of net photosynthesis by DBS was found.

The ^{18}O exchange technique also indicates the presence of light-dependent Ci transport systems. As shown in Fig. 4, illumination of 1,800 ppmv CO_2 grown cells of *S. costatum* and *P. globosa* resulted in a rapid uptake of ^{18}O-labeled $^{13}CO_2$ (m/z = 49 and 47) and a large efflux of unlabeled

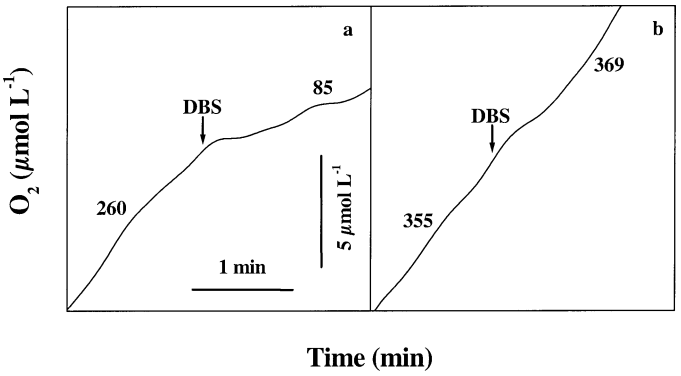

Fig. 3. Time course of photosynthetic O_2 evolution at (a) 3 μmol L^{-1} and (b) 27 μmol L^{-1} CO_2 in the absence and presence of DBS (100 μmol L^{-1}) for *S. costatum.* Addition of the inhibitor is indicated by arrows. Numbers close to the traces indicate the rate of O_2 evolution expressed as μmol (mg Chl *a*)$^{-1}$ h^{-1}.

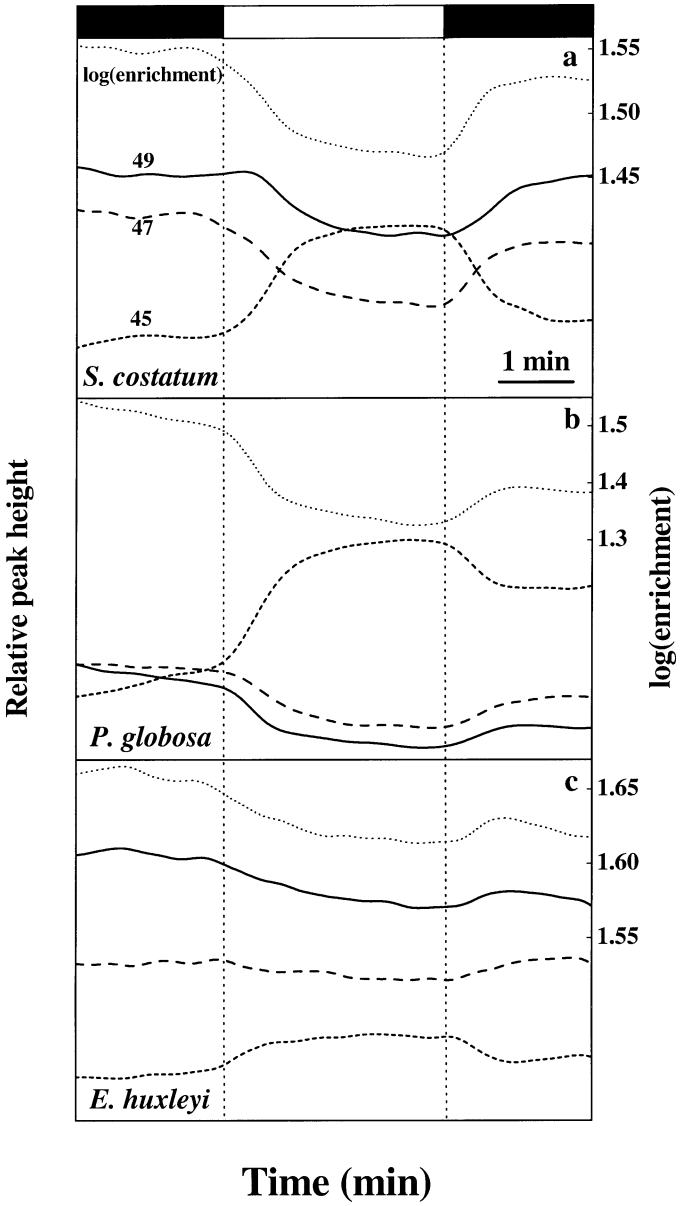

Fig. 4. Time course of changes in the relative concentrations of the CO_2 isotopes $^{13}C^{18}O_2$ (m/z = 49), $^{13}C^{16}O^{18}O$ (m/z = 47), $^{13}CO_2$ (m/z = 45) and the log (enrichment) by cells of (a) *S. costatum,* (b) *P. globosa,* and (c) *E. huxleyi.* The algae were either acclimated to 1,800 ppmv CO_2 (*S. costatum, P. globosa*) or 360 ppmv CO_2 (*E. huxleyi*). The eCA inhibitor DBS (100 μmol L^{-1}) was applied during the assay. Black and white bars at the top indicate the dark and light period, respectively. The figure shows representative data from at least three independent experiments.

$^{13}CO_2$ (m/z = 45), leading to a light-dependent decrease in log (enrichment) in both algae. In contrast, in *E. huxleyi* this light-stimulated decline in log (enrichment) was only observed in cells acclimated to 360 ppmv CO_2 and below.

Photosynthesis, CO_2 uptake, and HCO_3^- uptake—Net photosynthesis was measured by monitoring the O_2 evolution over several light–dark intervals with increasing Ci concentrations at constant pH. Simultaneous measurements of the

CO_2 concentration enabled us to estimate gross CO_2 uptake and HCO_3^- uptake kinetics according to equations by Badger et al. (1994). Net photosynthesis, gross CO_2 uptake, and HCO_3^- uptake are shown as a function of CO_2 and/or HCO_3^- concentration for *S. costatum*, *P. globosa*, and *E. huxleyi* (Figs. 5–7) acclimated to different pCO_2 levels. The corresponding kinetic parameters such as $K_{1/2}$ values and maximum rates (V_{max}) are summarized in Table 2. All species were able to take up both CO_2 and HCO_3^- during steady-state photosynthesis. However, large species-specific differences in the efficiency and regulation of carbon acquisition and photosynthesis are apparent.

In *S. costatum* $K_{1/2}$ values for photosynthetic O_2 evolution decreased from 2.7 to 0.3 μmol L^{-1} CO_2 (505 to 17 μmol L^{-1} HCO_3^-) with decreasing pCO_2 in the incubation, while V_{max} was unaffected by pCO_2 (Fig. 5; Table 2). The $K_{1/2}$ of gross CO_2 uptake decreased from 3.2 to 0.4 μmol L^{-1} CO_2 with decreasing pCO_2, and V_{max} remained relatively constant. The $K_{1/2}$ of HCO_3^- uptake decreased to 5 μmol L^{-1} HCO_3^-, and V_{max} strongly increased with decreasing pCO_2 in the incubation (48 to 239 μmol (mg Chl *a*)$^{-1}$ h^{-1}). In *P. globosa* $K_{1/2}$ values for photosynthetic O_2 evolution showed no consistent trend with pCO_2 and varied between 1.5 and 2.4 μmol L^{-1} CO_2 (122–175 μmol L^{-1} HCO_3^-), while the V_{max} increased slightly with decreasing pCO_2 in the incubation (Fig. 6; Table 2). The $K_{1/2}$ and V_{max} of gross CO_2 uptake remained unaffected by pCO_2 in the incubation, with $K_{1/2}$ showing values between 1.6 and 2.3 μmol L^{-1} CO_2. Likewise, HCO_3^- uptake kinetics did not change between the different pCO_2 incubation, except for a somewhat higher V_{max} at 36 ppmv pCO_2. In *E. huxleyi* $K_{1/2}$ values for photosynthetic O_2 evolution were much higher than of the other two species and decreased from 27.3 to 9.6 μmol L^{-1} CO_2 (1,646 to 581 μmol L^{-1} HCO_3^-) with decreasing pCO_2 in the incubation (Fig. 7, Table 2). The V_{max} of O_2 evolution was unaffected by pCO_2. For gross CO_2 uptake the $K_{1/2}$ decreased from 13.4 to 4.6 μmol L^{-1} CO_2 with decreasing pCO_2, while V_{max} remained relatively constant. The HCO_3^- uptake kinetics did not follow a Michaelis–Menten kinetic, but the HCO_3^- uptake rates relative to O_2 evolution slightly increased with decreasing pCO_2 in the incubation.

Discussion

In this study we investigated several aspects of inorganic carbon acquisition in ecologically relevant phytoplankton species by means of membrane inlet mass spectrometry. Acclimation to different pCO_2 levels was performed in unbuffered seawater with fairly low cell densities to match the natural environment as much as possible. The apparent $K_{1/2}$ values for photosynthetic O_2 evolution were significantly lower than values known for RubisCO (Badger et al. 1998), indicating the operation of a CCM. Moreover, all three species were able to use both CO_2 and HCO_3^- independently of the CO_2 concentration provided during growth. Despite these similarities, large differences in the efficiency and regulation of carbon acquisition become evident between species.

Carbonic anhydrase activity—Extracellular CA, which accelerates the conversion of HCO_3^- to CO_2 at the cell surface (Sültemeyer 1998), was found to increase in response to diminishing CO_2 supply in many microalgae, underlining the importance of eCA in carbon acquisition (e.g., Nimer et al. 1997; Elzenga et al. 2000; Burkhardt et al. 2001). The mass spectrometric measurement of eCA activity used in this study has the advantage that highly reproducible results can be obtained from living cells under growth temperature. Since eCA is the only CA that has access to *all* labeled Ci species in darkness, values for eCA activity indicate the acceleration in the rate by which the isotopic equilibrium is achieved and thus for changes in the rate of conversion between CO_2 and HCO_3^-.

In the present study *S. costatum* showed the strongest regulation and highest activity of eCA (Fig. 2). At 1,800 ppmv CO_2 activities of eCA were close to the detection limit but strongly increased with decreasing pCO_2 in the incubation. These results are consistent with the pH-dependent trends in eCA activity for *S. costatum* observed in other studies (Nimer et al. 1997, 1998). Potential light activation of eCA, as has been shown by Nimer et al. (1998), is not accounted for in our assay. For *S. costatum* they observed an increase in eCA activity at low CO_2 concentrations in the light compared to darkness, which was associated with higher redox activity of the plasma membrane. According to their findings the eCA activity obtained in our study could be higher at low CO_2 concentrations during illumination, which would potentially increase changes in eCA activity over the investigated [CO_2] range. For *P. globosa* we obtained high and relatively constant activities for eCA, indicating a constitutive rather than regulated system (Fig. 2). Elzenga et al. (2000) investigated the role of eCA in inorganic carbon use for *P. globosa* and found a gradual induction of eCA activity with decreasing CO_2 concentration over the duration of a bloom. Strain-specific differences in eCA activity, as known for example for *Phaeodactylum tricornutum* (John-McKay and Colman 1997; Burkhardt et al. 2001) or differences in carbon acquisition between single-celled flagellates (used in this study) and colonies of *P. globosa*, could be reasons for these apparent discrepancies. The eCA activities in *E. huxleyi* were very low and did not change with pCO_2 of the incubation (Fig. 2). Using an isotope disequilibrium method, Elzenga et al. (2000) could not detect any eCA activity for this strain of *E. huxleyi.* Nimer et al. (1994) investigated eCA activities of another high-calcifying strain by an electrometric method. They could not detect any eCA activity until *E. huxleyi* had reached the stationary phase. In contrast to the apparent role of eCA in carbon acquisition of *S. costatum* and *P. globosa*, eCA seems to play a minor role, if any, in this strain of *E. huxleyi.*

To further investigate a possible function of eCA on photosynthesis, we monitored O_2 evolution in the presence and absence of the CA inhibitor DBS at low (3 μmol L^{-1}) and high (27 μmol L^{-1}) CO_2 concentrations (Table 1, Fig. 4). DBS has previously been reported not to penetrate into the cells and, therefore, should inhibit only eCA activity. At 3 μmol L^{-1} CO_2, addition of DBS caused a strong reduction of O_2 evolution in 180 ppmv CO_2 acclimated cells of *S. costatum.* No such inhibitory effect of DBS on O_2 evolution was observed when photosynthesis was measured under 27 μmol L^{-1} CO_2 (Fig. 4). Similar results were obtained for

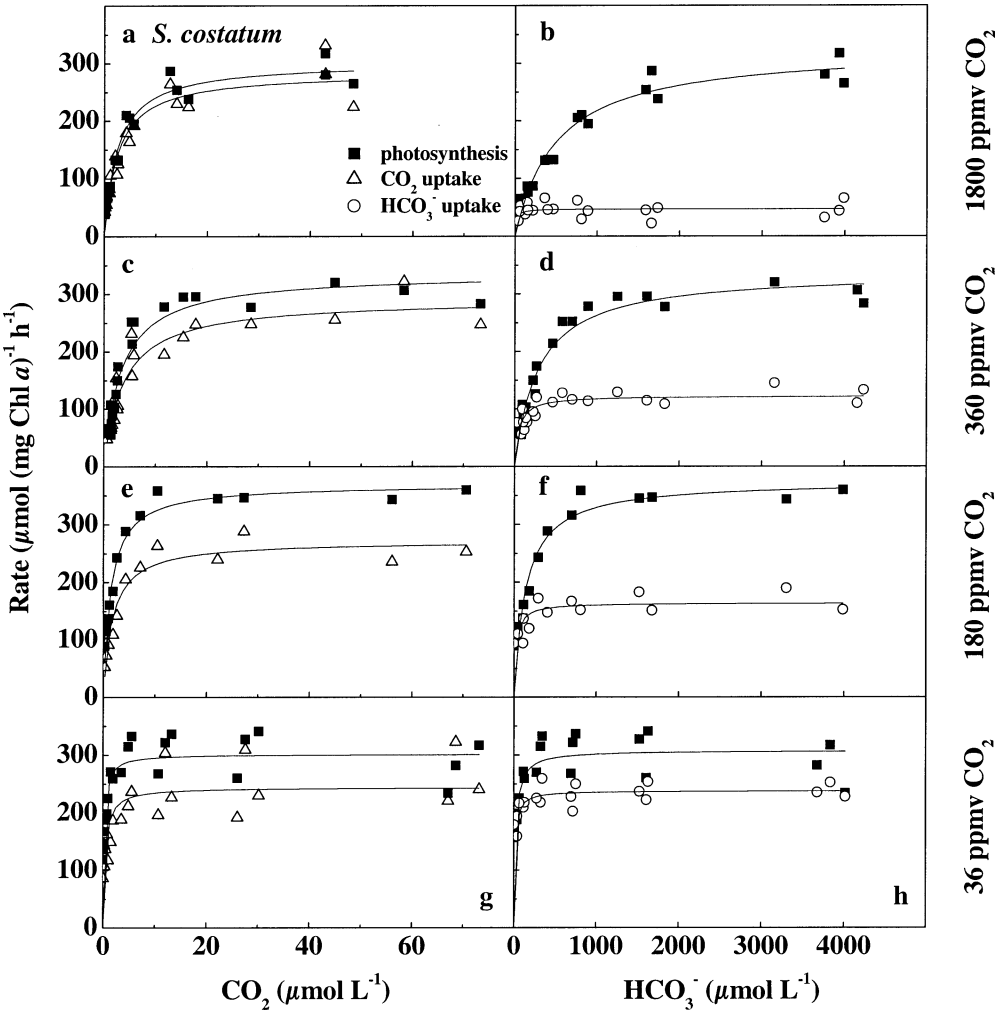

Fig. 5. *S. costatum.* Chl *a*–specific rates of net photosynthesis, gross CO_2 uptake, and HCO_3^- uptake as a function of CO_2 and HCO_3^- concentration in the assay medium. The cultures were acclimated to (a), (b) 1,800 ppmv, (c), (d) 360 ppmv, (e), (f) 180 ppmv, or (g), (h) 36 ppmv of CO_2 for at least 3 d. Curves were obtained from a Michaelis–Menten fit.

360 ppmv CO_2 grown cells of *S. costatum.* In contrast, in *P. globosa* significant DBS inhibition only occurred in 180 ppmv CO_2 acclimated cells (Table 1). In *E. huxleyi* addition of DBS had no effect on O_2 production (Table 1), which is consistent with the low eCA activities for this strain. The observed inhibition of O_2 evolution for *S. costatum* and *P. globosa* underlines the important role of eCA in carbon acquisition and supports earlier conclusions that eCA is essential for reaching maximum rates of photosynthesis under at least subsaturating CO_2 concentrations (Sültemeyer et al. 1990).

It is a common notion that eCA increases the CO_2 concentration at the plasma membrane and herewith favors CO_2 uptake. This only holds true, however, if low CO_2 concentrations in the boundary layer are the consequence of a disequilibrium in the carbonate system, as can occur during intense photosynthetic CO_2 fixation of large phytoplankton cells (Wolf-Gladrow and Riebesell 1997). For small algal cells, the expected disequilibrium due to photosynthetic CO_2 fixation is too small for eCA to significantly enhance CO_2 availability at the cell surface. For instance, assuming a 25-fold enhancement in the conversion of HCO_3^- to CO_2 (as determined by Elzenga et al. 2000) in the diffusive boundary layer of a 5-μm diameter algal cell growing at a rate of 1 d^{-1}, Riebesell and Wolf-Gladrow (2002) calculated an increase in the cell surface CO_2 concentration due to CA-catalyzed HCO_3^- conversion of only 0.04 μmol L^{-1}. Although this number increases to 0.25 μmol L^{-1} for a cell of 10-μm diameter, it is still small compared to the ambient CO_2 concentrations of $\sim$10 μmol L^{-1}. In view of these considerations it is puzzling, however, that the addition of CA to a culture of *E. huxleyi* (with a cell diameter of ca. 6 μm) resulted in a nearly 30% stimulation of photosynthesis in 2 mmol L^{-1} dissolved inorganic carbon and a pH of 8.1 (Sikes and Wheeler 1982). One possible explanation for the widespread occurrence of eCA in microalgae could be a direct involvement of this enzyme in an uptake system for CO_2 or HCO_3^- as suggested for cyanobacteria by Kaplan and Reinhold (1999).

The physiological role of intracellular CA, which can be

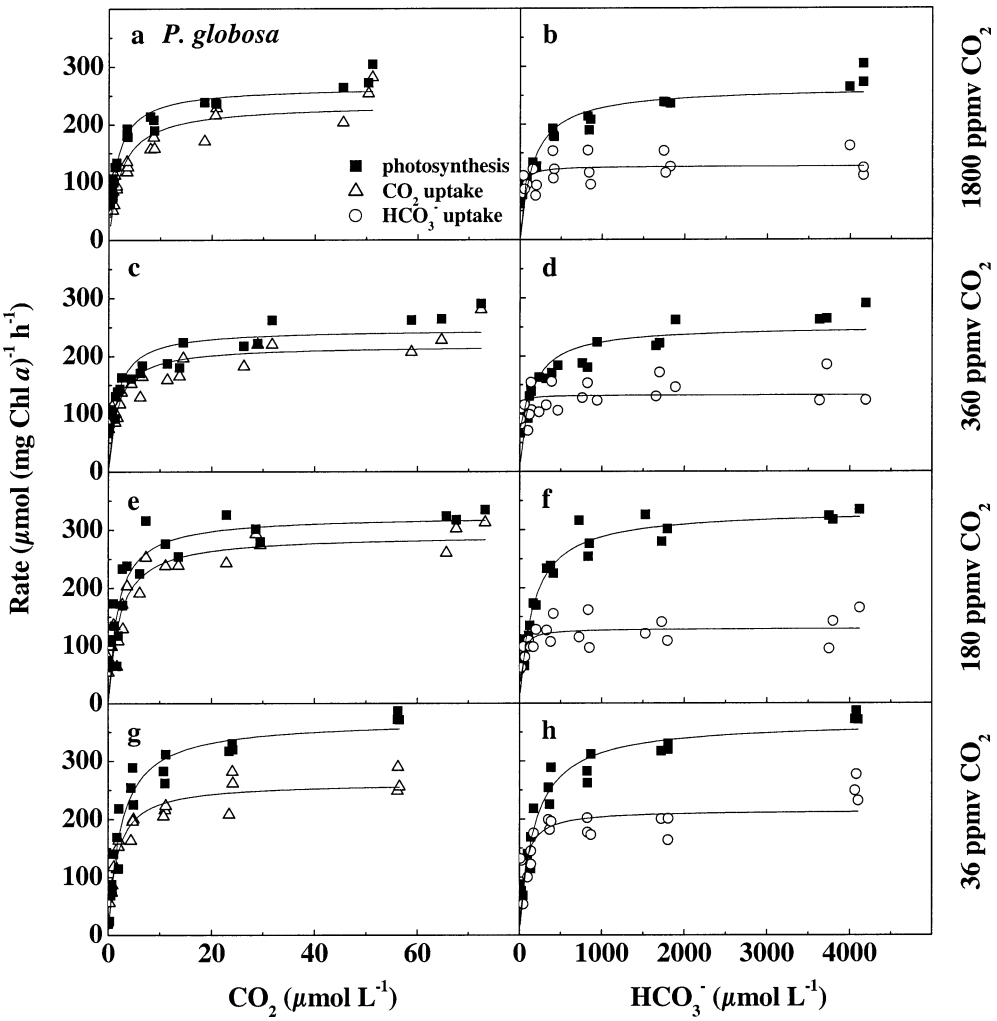

Fig. 6. *P. globosa.* Chl *a*–specific rates of net photosynthesis, gross CO_2 uptake, and HCO_3^- uptake as a function of CO_2 and HCO_3^- concentration in the assay medium. The cultures were acclimated to (a), (b) 1,800 ppmv, (c), (d) 360 ppmv, (e), (f) 180 ppmv, or (g), (h) 36 ppmv of CO_2 for at least 3 d. Curves were obtained from a Michaelis–Menten fit.

located in the chloroplast and the mitochondria, as well as the cytosol, remains unclear (Sültemeyer 1998). When interpreting iCA activities according to Palmqvist et al. (1994), one has to bear in mind that Δ values are dependent on the rate of diffusive CO_2 transport across cell membranes and the rate of extracellular and intracellular ^{18}O depletion. Figure 1 shows an example for the log (enrichment) of *P. globosa* acclimated to 36 ppmv CO_2. Since the same amount of cells were injected, the curves are directly comparable. As shown in this example, significantly different Δ values were obtained in the presence and absence of the eCA inhibitor DBS. In contrast with the results of Palmqvist et al. (1994), we therefore conclude that the eCA activity alters the estimates of and may even impose a trend on iCA activity. Although we used DBS in all iCA assays, Δ values remain arbitrary units, which allows direct comparison of different treatments but not between species. Results of Burkhardt et al. (2001) indicate a gradual increase in iCA activity of two marine diatoms in response to diminishing CO_2 supply. Our data do not confirm such a CO_2 dependence in iCA activity in the species tested since iCA activities increased at very low pCO_2 levels only for *S. costatum*. This may indicate that the response of iCA activity to reduced CO_2 levels is species dependent.

Light-stimulated ^{18}O exchange—Using the ^{18}O exchange technique, we examined the presence of light-dependent Ci transport systems. A potential influence by light activation of eCA (Nimer et al. 1998) was excluded by the presence of DBS during the assay. In the case of active Ci uptake, a large decline in log (enrichment) during illumination would be expected, which is caused by an enhanced influx of ^{18}O-labeled CO_2 and HCO_3^- into the cells to the active site of intracellular CA, increased ^{18}O loss, and subsequent efflux of ^{18}O unlabeled CO_2 (Badger and Price 1989; Palmqvist et al. 1994). Such a net CO_2 efflux from photosynthetically active cells due to leakage through the cell membrane can be explained by accumulation of CO_2 inside the cell relative to ambient CO_2 concentration. As shown in Fig. 4, illumination of 1,800 ppmv CO_2 grown cells of *S. costatum* and

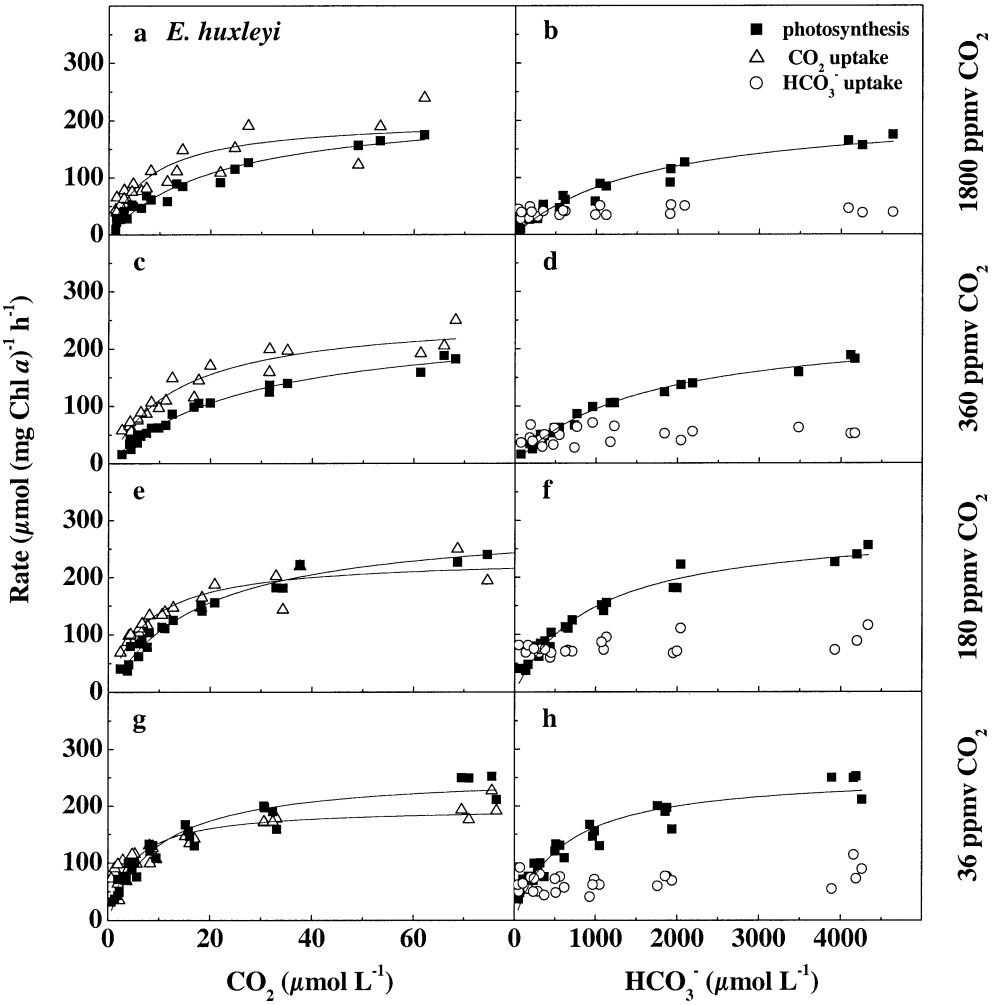

Fig. 7. *E. huxleyi*. Chl *a*–specific rates of net photosynthesis, gross CO_2 uptake, and HCO_3^- uptake as a function of CO_2 and HCO_3^- concentration in the assay medium. The cultures were acclimated to (a), (b) 1,800 ppmv, (c), (d) 360 ppmv, (e), (f) 180 ppmv, or (g), (h) 36 ppmv of CO_2 for at least 3 d. Curves were obtained from a Michaelis–Menten fit.

P. globosa resulted in a rapid uptake of $^{13}C^{18}O_2$ (m/z = 49) and a large efflux of $^{13}CO_2$ (m/z = 45), i.e., a light-dependent decrease in log (enrichment). The involvement of a rapid induction of eCA activity (Nimer et al. 1998) in this process can be ruled out since we added DBS to the reaction assay in order to inhibit eCA. A likely explanation of the observed changes in ^{18}O exchange therefore is the presence of CCM associated Ci uptake systems even in cells grown under elevated CO_2 concentrations. The apparently greater lag phase for *S. costatum* could be explained by a lower leakage or slower induction of the Ci uptake in this species. In *E. huxleyi* the light-stimulated ^{18}O exchange is not present in 1,800 ppmv CO_2 grown cells (not shown) and far less pronounced in cells acclimated to 360 ppmv CO_2 (Fig. 4), which indicates that Ci transport in this species is only induced at lower CO_2 levels.

Photosynthetic O_2 evolution—Monitoring photosynthetic O_2 evolution as a function of CO_2 concentration provides important information about the carbon acquisition of microalgae. CO_2-induced changes and generally lower $K_{1/2}$ (CO_2) values than K_M $(CO_2)_{RubisCO}$ indicate the operation of a CCM. *S. costatum* strongly regulates its CCM, which is shown by the large changes in $K_{1/2}$ for photosynthesis (Fig. 5; Table 2). According to our results *P. globosa* has a highly efficient CCM but apparently does not regulate in response to CO_2 supply as indicated by more or less constant values of $K_{1/2}$ for O_2 evolution over a wide range of pCO_2 (Fig. 6, Table 2). The high values of $K_{1/2}$ for *E. huxleyi* (Fig. 7, Table 2) imply that photosynthesis in this species is not even carbon saturated under conditions commonly found in the ocean. Nevertheless, *E. huxleyi* showed some degree of regulation in its carbon acquisition, which is shown by the CO_2-induced changes in the $K_{1/2}$. The operation of a CCM in this strain of *E. huxleyi* was previously predicted from $\delta^{13}C$ isotope fractionation experiments by Rost et al. (2002). Another highly calcifying strain of *E. huxleyi* was shown to induce a CCM toward the stationary phase (Nimer and Merrett 1996).

The efficiency of a CCM may be assessed from the ratio

Table 2. $K_{½}$ and V_{max} of photosynthesis, gross CO_2 uptake, and HCO_3^- uptake for *S. costatum, P. globosa,* and *E. huxleyi* acclimated at different pCO_2. Kinetic parameters were calculated from a Michaelis–Menten fit to the combined data of several independent measurements. Values for $K_{½}$ and V_{max} are given in μmol L^{-1} and μmol (mg Chl *a*)$^{-1}$ h^{-1}, respectively. Error bars denote ±SD.

	Photosynthesis				CO_2 uptake		HCO_3^-	
pCO_2 (ppmv)	$K_{½}$ (CO_2)	V_{max} (CO_2)	$K_{½}$ (HCO_3)	V_{max} (HCO_3)	$K_{½}$ (CO_2)	V_{max} (CO_2)	$K_{½}$ (HCO_3)	V_{max} (HCO_3)
S. costatum								
1800	2.7 ± 0.4	322 ± 13	505 ± 87	347 ± 19	2.3 ± 0.4	283 ± 14	—	48 ± 11
360	2.3 ± 0.5	341 ± 21	246 ± 40	353 ± 16	3.2 ± 0.9	299 ± 23	38 ± 14	115 ± 6
180	1.4 ± 0.1	369 ± 9	138 ± 29	374 ± 18	1.8 ± 0.3	271 ± 12	24 ± 14	164 ± 13
36	0.3 ± 0.1	314 ± 13	17 ± 5	316 ± 10	0.4 ± 0.1	259 ± 15	5 ± 2	239 ± 6
P. globosa								
1800	1.6 ± 0.2	265 ± 8	154 ± 38	264 ± 14	2.3 ± 0.5	235 ± 13	18 ± 9	127 ± 9
360	1.5 ± 0.4	246 ± 13	122 ± 29	251 ± 13	1.7 ± 0.5	218 ± 15	23 ± 13	133 ± 7
180	1.8 ± 0.4	323 ± 18	161 ± 21	334 ± 11	2.1 ± 0.5	291 ± 16	23 ± 8	130 ± 6
36	2.4 ± 0.3	370 ± 13	175 ± 30	369 ± 5	1.6 ± 0.3	262 ± 9	56 ± 24	215 ± 15
E. huxleyi								
1800	21.7 ± 3.3	225 ± 16	1646 ± 329	220 ± 14	7.9 ± 2.1	204 ± 20	—	43 ± 8
360	27.3 ± 2.4	250 ± 11	1562 ± 147	245 ± 13	13.4 ± 1.9	260 ± 14	—	58 ± 15
180	18.2 ± 1.7	298 ± 11	958 ± 108	291 ± 11	7.0 ± 1.1	235 ± 11	—	79 ± 10
36	9.6 ± 1.2	257 ± 11	581 ± 87	257 ± 15	4.6 ± 0.8	197 ± 10	—	67 ± 14

between K_M (CO_2) of RubisCO and the apparent $K_{1/2}$ (CO_2) of O_2 evolution. This ratio approximates the enrichment in internal [CO_2] at the site of RubisCO compared to the ambient [CO_2]. For our calculations we used previously reported K_M values for RubisCO (Badger et al. 1998) and $K_{1/2}$ values obtained in this study (Table 2). While the K_M:$K_{1/2}$ ratio increased with decreasing CO_2 concentrations in incubations of *S. costatum* and *E. huxleyi*, it showed no trend for *P. globosa* (Fig. 8a), again indicating that the latter species does not regulate its CCM in relation to external CO_2 concentrations. *S. costatum* reached the highest values of up to 120, whereas K_M:$K_{1/2}$ ratios of *E. huxleyi* ranged between 1 and 3. These results are consistent with the observed species-specific patterns of light-stimulated ^{18}O exchange. Although the CO_2 dependence in O_2 evolution reveals information about the efficiency and regulation of the CCM, it cannot provide any details about the underlying mechanisms.

Carbon uptake kinetics—Various methods have been employed to distinguish between CO_2 and HCO_3^- uptake in microalgae. In this study estimates of CO_2 and HCO_3^- uptake rates were obtained by a method of Badger et al. (1994), which has the advantage that inorganic carbon fluxes can be quantified at steady-state photosynthesis. While this method has successfully been applied to cyanobacteria and several freshwater microalgae (Badger et al. 1994; Tchernov et al. 1997; Amoroso et al. 1998), it has only recently been used to examine two marine diatoms (Burkhardt et al. 2001). Our observation of simultaneous CO_2 and HCO_3^- uptake for marine phytoplankton is consistent with the results of previous studies (e.g., Colman and Rotatore 1995; Burkhardt et al. 2001). The uptake kinetics for both substrates differ strongly between the investigated species (Table 2).

In *S. costatum* the CO_2 and HCO_3^- uptake systems showed high affinities even at 1,800 ppmv CO_2, which increased even more with decreasing pCO_2 in the incubation (Fig. 5). Concomitantly, the contribution of HCO_3^- to the overall carbon acquisition increased. A possible explanation for the increase in substrate affinity could either be posttranslational regulation (Sültemeyer et al. 1998) or an increasing expression of a high affinity uptake system, as has already been suggested for cyanobacteria (Shibata et al. 2002). The larger contribution of HCO_3^- is the result of an increasing number of transport components with decreasing CO_2 concentrations. Direct uptake of HCO_3^- has previously been suggested for *S. costatum* (Korb et al. 1997) but has hitherto not been quantified.

In *P. globosa*, the affinities of the CO_2 and HCO_3^- uptake system were high and showed no trend with pCO_2 in the incubation (Fig. 6), which is consistent with our results for O_2 evolution. Elzenga et al. (2000) concluded from their results that *P. globosa* uses HCO_3^- by means of CA-mediated conversion to CO_2, which then diffuses across the membrane. The high activities of eCA and the inhibition of O_2 evolution by DBS observed in our study are generally consistent with a CA-mediated use of HCO_3^- in addition to direct uptake of HCO_3^-. A preference for CO_2 as the substrate of *P. globosa* is also indicated by the characteristics of CO_2 and O_2 changes during the measurement, showing a higher rate of O_2 evolution at the beginning of the light interval when CO_2 concentration is still higher (data not shown). Nevertheless, it could be shown that *P. globosa* is able to take up HCO_3^- directly, and this system contributes significantly to the overall carbon acquisition. One has to consider, however, that a prerequisite of the carbon flux measurement is the absence of eCA activity. In the presence of eCA activity the proportion of direct HCO_3^- uptake to the overall carbon acquisition might be smaller because of an increasing indirect use of HCO_3^-. In contrast to the results of Elzenga et al. (2000), we did not find a gradual induction in HCO_3^- use. Yet it seems that direct HCO_3^- uptake and eCA-mediated HCO_3^- use are more pronounced in the lowest pCO_2 incubation.

The high $K_{1/2}$ values for O_2 evolution of *E. huxleyi* are

reflected in the relatively low affinities of the CO_2 uptake system. The uptake of HCO_3^- could not be described by Michaelis–Menten kinetics, which is consistent with findings of Nimer and Merrett (1992). While the CO_2 uptake system largely reflects the kinetics of the O_2 evolution, the HCO_3^- uptake seems to provide a constant background flux of inorganic carbon. The latter may point to an involvement of the calcification process in HCO_3^- use of *E. huxleyi*. It has previously been suggested that calcifying strains of *E. huxleyi* are able to produce CO_2 by the process of calcification, which is then used for photosynthetic C fixation (e.g., Sikes et al. 1980; Nimer and Merrett 1992). Coccolith formation in *E. huxleyi* could thereby serve to partly compensate for the low efficiency of its CCM. The extent to which photosynthesis and calcification are linked and whether calcification supports photosynthetic carbon acquisition is still under debate.

To mimic natural seawater carbonate chemistry we did not add any artificial buffer to the culture media. As pointed out by Burkhardt et al. (2001), buffers have a pronounced effect on the carbonate system as they keep the ratio of $[HCO_3^-]$:$[CO_2]$ constant despite changes in pCO_2. In natural seawater, changes in CO_2 concentration are accompanied by respective changes in pH and the $[HCO_3^-]:[CO_2]$ ratio. In our experiments, changes in pCO_2 from 36 to 1,800 ppmv resulted in a decrease in pH from 9.1 to 7.6 and a decrease in $[HCO_3^-]$:$[CO_2]$ ratio from 767 to 32, respectively. Using uptake kinetics obtained in this study and the corresponding carbonate system speciation for each of the pCO_2 incubations we calculated the ratio of gross CO_2 to HCO_3^- uptake (Fig. 8b). Values larger than 1 indicate a preference for CO_2, values below 1 a preference for HCO_3^- as carbon source. While the three species take up both CO_2 and HCO_3^- over the entire range of CO_2 concentrations tested, CO_2 was the preferred substrate in all but the lowest CO_2 incubation. Under air-equilibrated CO_2 concentrations, the cells take up about twice as much CO_2 as HCO_3^-. A gradual induction of HCO_3^- uptake occurred with decreasing pCO_2 in the incubation, with *S. costatum* showing the largest and *P. globosa* the smallest changes between treatments.

The calculation of these uptake ratios is based on the assumption that the CO_2 and HCO_3^- uptake systems are regulated independently of each other and that changes in pH have no significant effect on uptake kinetics. Unlike the conditions in our pCO_2 controlled incubations, the $[HCO_3^-]$:$[CO_2]$ ratio in the assays remained constant. If this ratio has an effect on the regulation of the different uptake systems, the calculations would lead to erroneous estimates of uptake kinetics in the culture. Microalgae with a preference for CO_2, for instance, might cover a larger proportion of their total inorganic carbon uptake by CO_2 at the low $[HCO_3^-]:[CO_2]$ ratio of a high pCO_2 culture (pH 7.6) than under the higher $[HCO_3^-]:[CO_2]$ ratio in the assay (pH 8.0). Another critical point is that the gross CO_2 uptake might be underestimated as a result of cell compartmentation (Badger et al. 1994). An increased CA-mediated HCO_3^- use, which is inhibited in the assay by DBS, could decrease the direct uptake of HCO_3^-. All of these factors would lead to an increase in the $CO_2:HCO_3^-$ uptake rates compared to our calculated values. In other words, the calculation could underestimate the contribution of CO_2. The presence of HCO_3^- leakage, as suggested by Tchernov et al. (1997), however, would increase HCO_3^- uptake rates and thus decrease the $CO_2:HCO_3^-$ uptake ratio. For an in-depth assessment of these methodological uncertainties we refer to Badger et al. (1994), Kaplan and Reinhold (1999), and Burkhardt et al. (2001).

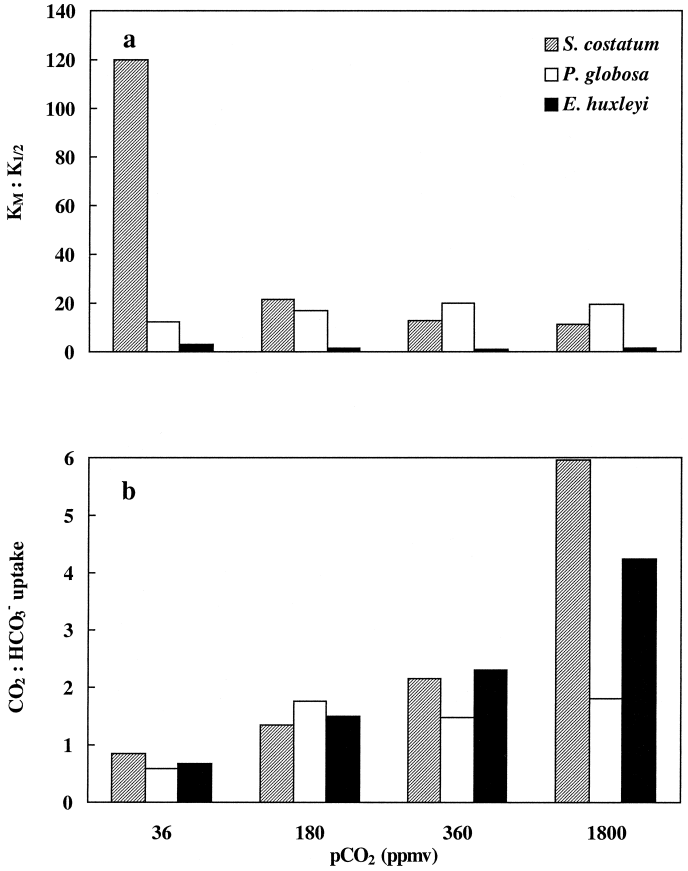

Fig. 8. Ratios of (a) $K_M(CO_2)_{Rubisco}:K_{1/2}$ (CO_2) for O_2 evolution and (b) gross $CO_2:HCO_3^-$ uptake in *S. costatum*, *P. globosa*, and *E. huxleyi*, acclimated to different pCO_2 in the culture medium. $K_M(CO_2)_{Rubisco}$ was assumed to be 30 μmol L^{-1} (Badger et al. 1998).

Ecological and biogeochemical implications—Although most phytoplankton species reach photosynthetic saturation under ambient CO_2 levels (Raven and Johnston 1991), this does not imply that species are equally efficient in their carbon acquisition. In fact, phytoplankton species differ significantly in the extent to which they actively transport HCO_3^- and/or CO_2 and accumulate inorganic C intracellularly (Raven 1997; Badger et al. 1998). As pointed out by Tortell (2000), the efficiency of the CCM of different taxonomic groups seems to be negatively correlated with the catalytic efficiency of their RubisCO. Our results indicate large differences in both efficiency and regulation of inorganic carbon acquisition for representatives of three phytoplankton functional groups. These differences may affect the relative fitness of the different groups and thus could help to explain the distribution and succession of phytoplankton in space and time.

Microalgae with regulated CCMs can optimize the allo-

cation of resources for operating carbon acquisition mechanisms in response to changing growth conditions. Part of this regulation is the observed preference for CO_2 under elevated CO_2 concentrations, since CO_2 uptake is considered to be less costly than HCO_3^- uptake (Raven 1990). Under severe CO_2 limitation, however, HCO_3^- uptake becomes increasingly important despite presumably higher costs. Consistent with the cost–benefit strategy is also the up-regulation of the eCA activities as CO_2 concentrations decrease. CCM activity is also influenced by the energy (light) supply. For example, light limitation was found to decrease the capacity of Ci transport (Shiraiwa and Miyachi 1983; Beardall 1991). Based on carbon isotope fractionation experiments, Rost et al. (2002) proposed that both photon flux density and daylength influence the regulation of active carbon uptake in *E. huxleyi*, presumably by modulating the Ci demand of the cell. In fact, the duration of the photoperiod was shown to influence the operation of the CCM in the three species tested in this study (Rost et al. unpubl.).

Despite the ability of most phytoplankton species to regulate their carbon acquisition, large differences exist in the efficiencies. Owing to their highly efficient CCMs, photosynthetic carbon fixation rates of all diatom species tested so far, as well as of *P. globosa*, are at or close to CO_2 saturation at present day CO_2 levels (e.g., Raven and Johnston 1991; Burkhardt et al. 2001; this study). In contrast, coccolithophorids such as *E. huxleyi* seem to be well below saturation at these levels (Paasche 1964; Nielsen 1995; Riebesell et al. 2000; this study) and thus are more CO_2 sensitive. In fact, although the cell division rate of *E. huxleyi* remains more or less constant over a wide range of CO_2 concentrations, carbon fixation rate and carbon-specific growth rate are strongly CO_2 dependent (Paasche et al. 1996; Rost et al. 2002), reflecting the low efficiency of its CCM.

According to the ecological aspects discussed above, differences in inorganic carbon acquisition may play a role for the competitive advantage of marine phytoplankton. Bloom-forming species should be especially dependent on a regulated and efficient CCM, since they must maintain high growth rates even under conditions in a bloom, when CO_2 concentrations decrease due to photosynthetic carbon consumption (down to ~ 5 μmol L^{-1}). By the end of this century, the expected increase in the atmospheric CO_2 will give rise to an almost threefold increase in surface water CO_2 concentrations relative to preindustrial values. This will cause the $[HCO_3^-]:[CO_2]$ ratio and seawater pH to decrease by ca. 65% and 0.35 units, respectively (Wolf-Gladrow et al. 1999). These changes are likely to affect phytoplankton, yet in different ways. Microalgae that react to ambient CO_2 concentrations, as shown for *S. costatum* and *E. huxleyi*, may have advantages in the future compared to preindustrial or glacial times owing to the potential reduction in their CCMs. Phytoplankton productivity based on carbon or energy content might therefore increase under typically resource-limiting conditions in the ocean (Raven and Johnston 1991). CO_2-sensitive coccolithophorids such as *E. huxleyi* may benefit even more from the present increase in atmospheric CO_2 when compared to diatoms and *Phaeocystis*. Since coccolithophorid blooms predominantly occur in well-stratified waters that are expected to extend and intensify in the future (Sarmiento et al. 1998), projected climate-induced changes in the marine environment may prove even more advantageous for this group of phytoplankton.

According to the functional group concept (Falkowski et al. 1998) diatoms, *Phaeocystis*, and coccolithophorids each play a specific role in the marine ecosystem and have distinct effects on elemental cycling. One of the most prominent examples is the differential impact of calcifying and noncalcifying phytoplankton on the CO_2 air–sea exchange. While the latter drive the organic carbon pump, which causes a draw down of CO_2 in the surface ocean, the former also contribute to the calcium carbonate pump, which releases CO_2 into the environment (Robertson et al. 1994). As discussed above, rising CO_2 levels and increasing stratification might increase the contribution of the calcifying phytoplankton to overall primary production, which consequently would increase the ratio of calcification to organic carbon production. An increase in this ratio, which might result from an increased contribution of coccolithophorids, would enhance the relative strength of the carbonate pump. This in turn would lower the biologically mediated CO_2 uptake from the atmosphere. A basin-wide shift in the composition of sediment particles, as indicated by a decrease of the opal : carbonate ratio, has in fact been observed across the entire North Atlantic and is suggested to be related to large-scale changes in climate forcing (Antia et al. 2001). These findings are consistent with high concentrations of coccoliths observed in interglacial sediments, whereas glacial sediments are poor in biogenic carbonate (e.g., Henrich 1989).

On the other hand, there are indications that rising atmospheric CO_2 may affect marine biogenic calcification in yet another way. Rates of calcification of dominant calcifying organisms such as corals, foraminifera, and coccolithophorids were shown to decrease under elevated CO_2 concentrations (Kleypas et al. 1999; Bijma et al. 1999; Riebesell et al. 2000). A CO_2-related reduction in calcification decreases the ratio of calcification to organic matter production. With ca. 80% of the global $CaCO_3$ production contributed by planktonic organisms, reduced calcification decreases the strength of the calcium carbonate pump and thereby increases the biologically driven draw down of CO_2 by the surface ocean (Zondervan et al. 2001). The climate-induced increase in the contribution of coccolithophorids to total primary production and a CO_2-related decrease in biogenic calcification would have opposing effects on the marine carbon cycle. Their net effect on carbon cycling will depend on their relative importance and sensitivity to global change. Changes in marine production, phytoplankton species composition, and succession will also impact other biogeochemical cycles, such as nitrogen, opal, and sulfur cycles, which in turn is bound to feed back on the climate.

In conclusion, the results of this study revealed species-specific differences in CO_2-dependent photosynthetic O_2 evolution, substrate affinities, relative contribution of HCO_3^- to total carbon uptake and eCA activity as well as differences in the degree of pCO_2-dependent regulation. Our results indicate a highly efficient and regulated carbon acquisition for *S. costatum*, which can be ascribed to increasing affinities in the CO_2 and HCO_3^- uptake systems, an increasing contribution of HCO_3^- to the overall carbon acquisition,

and an increase in eCA activity with decreasing pCO_2. *P. globosa* showed a highly efficient but rather constitutive carbon acquisition, which was reflected in the high affinities of the CO_2 and HCO_3^- uptake systems, a constant contribution of HCO_3^- to the overall carbon acquisition, and high eCA activities independent of the pCO_2. For *E. huxleyi* an inefficient albeit regulated carbon acquisition was observed, with low affinities in the inorganic carbon uptake systems and low eCA activities. If observed differences between these species are representative for the corresponding phytoplankton functional groups in the natural environment, CO_2-related changes in seawater chemistry are expected to modify phytoplankton species succession and distribution. Responses in phytoplankton communities, especially shifts in the dominance between functional groups, are likely to influence biogeochemical cycling. Effects of elevated CO_2 on the physiology and ecology of phytoplankton have to be assessed in more detail, especially with respect to their feedback on ecosystem regulation and global biogeochemical cycles.

References

AMOROSO, G., D. SÜLTEMEYER, C. THYSSEN, AND H. P. FOCK. 1998. Uptake of HCO_3^- and CO_2 in cells and chloroplasts from the microalgae *Chlamydomonas reinhardtii* and *Dunaliella tertiolecta.* Plant Physiol. **116:** 193–201.

ANTIA, A. N., AND OTHERS. 2001. Basin-wide particulate carbon flux in the Atlantic Ocean: Regional export patterns and potential for atmospheric CO_2 sequestration. Glob. Biogeochem. Cycles **15:** 845–862.

BADGER, M. R., T. J. ANDREWS, S. M. WHITNEY, M. LUDWIG, D. C. YELLOWLEES, W. LEGGAT, AND G. D. PRICE. 1998. The diversity and coevolution of Rubisco, plastids, pyrenoids, and chloroplast-based CO_2-concentrating mechanisms in algae. Can. J. Bot. **76:** 1052–1071.

———, K. PALMQVIST, AND J.-W. YU. 1994. Measurement of CO_2 and HCO_3^- fluxes in cyanobacteria and microalgae during steady-state photosynthesis. Physiol. Plant. **90:** 529–536.

———, AND G. D. PRICE. 1989. Carbonic anhydrase activity associated with the cyanobacterium *Synechococcus* PCC7942. Plant Physiol. **89:** 51–60.

BEARDALL, J. 1991. Effects of photon flux density on the 'CO_2-concentrating mechanism' of the cyanobacterium *Anabaena variabilis.* J. Res. **13:** 133–141.

BIJMA, J., H. J. SPERO, AND D. W. LEA. 1999. Reassessing foraminiferal stable isotope geochemistry: Impact of the oceanic carbonate system (experimental results), p. 489–512. *In* G. Fischer and G. Wefer [eds.], Use of proxies in paleoceanography: Examples from the South Atlantic. Springer.

BURKHARDT, S., G. AMOROSO, U. RIEBESELL, AND D. SÜLTEMEYER. 2001. CO_2 and HCO_3^- uptake in marine diatoms acclimated to different CO_2 concentrations. Limnol. Oceanogr. **46:** 1378–1391.

COLMAN, B., AND C. ROTATORE. 1995. Photosynthetic inorganic carbon uptake and accumulation in two marine diatoms. Plant Cell Environ. **18:** 919–924.

ELZENGA, J. T. M., H. B. A. PRINS, AND J. STEFELS. 2000. The role of extracellular carbonic anhydrase activity in inorganic carbon utilization of *Phaeocystis globosa* (Prymnesiophyceae): A comparison with other marine algae using the isotope disequilibrium technique. Limnol. Oceanogr. **45:** 372–380.

FALKOWSKI, P. G., R. T. BARBER, AND V. SMETACEK. 1998. Biogeochemical controls and feedbacks on ocean primary production. Science **281:** 200–206.

———, AND J. A. RAVEN. 1997. Aquatic photosynthesis. Blackwell.

GOYET, C., AND A. POISSON. 1989. New determination of acid dissociation constants in seawater as a function of temperature and salinity. Deep-Sea Res. **36:** 1635–1654.

GRAN, G. 1952. Determination of the equivalence point in potentiometric titrations of seawater with hydrochloric acid. Oceanol. Acta **5:** 209–218.

GUILLARD, R. R. L., AND J. H. RYTHER. 1962. Studies of marine planktonic diatoms. Can. J. Microbiol. **8:** 229–239.

HENRICH, R. 1989. Diagenetic environments of authigenic carbonates and opal-ct crystallization in Lower Miocene to Upper Oligocene Deposits of the Norwegian Sea (ODP Site 643, Leg 104), p. 233–248. *In* O. Eldholm, J. Thiede, and E. Taylor [eds.], Proceedings of the Ocean Drilling Program. Vol. 104, Scientific Results.

JOHN-MCKAY, M. E., AND B. COLMAN. 1997. Variation in the occurrence of external carbonic anhydrase among strains of the marine diatom *Phaeodactylum tricornutum* (Bacillariophyceae). J. Phycol. **33:** 988–990.

JOHNSON, K. M., K. D. WILLS, D. B. BUTLER, W. K. JOHNSON, AND C. S. WONG. 1993. Coulometric total carbon dioxide analysis for marine studies: Maximizing the performance of an automated gas extraction system and coulometric detector. Mar. Chem. **44:** 167–187.

KAPLAN, A., AND L. REINHOLD. 1999. CO_2 concentrating mechanisms in photosynthetic microorganisms. Annu. Rev. Plant Physiol. Plant Mol. Biol. **50:** 539–570.

KLEYPAS, J. A., R. W. BUDDEMEIER, D. ARCHER, J.-P. GATTUSO, C. LANGDON, AND B. N. OPDYKE. 1999. Geochemical consequences of increased atmospheric CO_2 on coral reefs. Science **284:** 118–120.

KORB, R. E., P. J. SAVILLE, A. M. JOHNSTON, AND J. A. RAVEN. 1997. Sources of inorganic carbon for photosynthesis by three species of marine diatom. J. Phycol. **33:** 433–440.

NIELSEN, M. V. 1995. Photosynthetic characteristics of the coccolithophorid *Emiliania huxleyi* (Prymnesiophyceae) exposed to elevated concentrations of dissolved inorganic carbon. J. Phycol. **31:** 715–719.

NIMER, N. A., Q. GUAN, AND M. J. MERRETT. 1994. Extra- and intra-cellular carbonic anhydrase in relation to culture age in a high-calcifying strain of *Emiliania huxleyi* Lohmann. New Phytol. **126:** 601–607.

———, M. D. IGLESIAS-RODRIGUEZ, AND M. J. MERRETT. 1997. Bicarbonate utilization by marine phytoplankton species. J. Phycol. **33:** 625–631.

———, AND M. J. MERRETT. 1992. Calcification and utilization of inorganic carbon by the coccolithophorid *Emiliania huxleyi* Lohmann. New Phytol. **121:** 173–177.

———, AND ———. 1996. The development of a CO_2-concentrating mechanism in *Emiliania huxleyi.* New Phytol. **133:** 383–389.

———, M. WARREN, AND M. J. MERRETT. 1998. The regulation of photosynthetic rate and activation of extracellular carbonic anhydrase under CO_2-limiting conditions in the marine diatom *Skeletonema costatum.* Plant Cell Environ. **21:** 805–812.

PAASCHE, E. 1964. A tracer study of the inorganic carbon uptake during coccolith formation and photosynthesis in the coccolithophorid *Coccolithus huxleyi.* Physiol. Plant. Suppl. **3:** 1–82.

———, S. BRUBAK, S. SKATTEBØL, J. R. YOUNG, AND J. C. GREEN. 1996. Growth and calcification in the coccolithophorid *Emiliania huxleyi* (Haptophyceae) at low salinities. Phycologia **35:** 394–403.

PALMQVIST, K., J.-W. YU, AND M. R. BADGER. 1994. Carbonic an-

hydrase activity and inorganic carbon fluxes in low- and high-Ci cells of *Chlamydomonas reinhardtii* and *Scenedesmus obliquus.* Physiol. Plant. **90:** 537–547.

RAVEN, J. A. 1990. Predictions of Mn and Fe use efficiencies of phototrophic growth as a function of light availability for growth. New Phytol. **116:** 1–18.

———. 1997. Inorganic carbon acquisition by marine autotrophs. Adv. Bot. Res. **27:** 85–209.

———, AND A. M. JOHNSTON. 1991. Mechanisms of inorganic-carbon acquisition in marine phytoplankton and their implications for the use of other resources. Limnol. Oceanogr. **36:** 1701–1714.

RIEBESELL, U., AND D. A. WOLF-GLADROW. 2002. Supply and uptake of inorganic nutrients, p. 109–140. *In* P. J. le B. Williams, D. N. Thomas, and C. S. Reynolds [eds.], Phytoplankton productivity—carbon assimilation in marine and freshwater ecosystems. Blackwell Science.

———, I. ZONDERVAN, B. ROST, P. D. TORTELL, R. E. ZEEBE, AND F. M. M. MOREL. 2000. Reduced calcification in marine plankton in response to increased atmospheric CO_2. Nature **407:** 634–637.

ROBERTSON, J. E., AND OTHERS. 1994. The impact of a coccolithophore bloom on oceanic carbon uptake in the northeast Atlantic during summer 1991. Deep-Sea Res. **41:** 297–314.

ROST, B., I. ZONDERVAN, AND U. RIEBESELL. 2002. Light-dependent carbon isotope fractionation in the coccolithophorid *Emiliania huxleyi.* Limnol. Oceanogr. **47:** 120–128.

SARMIENTO, J. L., T. M. C. HUGHES, R. J. STOUFFER, AND S. MANABE. 1998. Simulated response of the carbon cycle to anthropogenic climate warming. Nature **393:** 245–249.

SHIBATA, M., H. OHKAWA, H. KATOH, M. SHIMOYAMA, AND T. OGAWA. 2002. Two CO_2 uptake systems in cyanobacteria: Four systems for inorganic carbon acquisition in *Synechocystis* sp. Strain PCC6803. Funct. Plant Biol. **29:** 123–129.

SHIRAIWA Y., AND S. MIYACHI. 1983. Factors controlling induction of carbonic anhydrase and efficiency of photosynthesis in *Chlorella vulgaris* 11h cells. Plant Cell Physiol. **26:** 919–923.

SIKES, C. S., R. D. ROER, AND K. M. WILBUR. 1980. Photosynthesis and coccolith formation: Inorganic carbon sources and net inorganic reaction of deposition. Limnol Oceanogr. **25:** 248–261.

———, AND A. P. WHEELER. 1982. Carbonic anhydrase and carbon fixation in coccolithophorids. J. Phycol. **18:** 423–426.

SILVERMAN, D. N. 1982. Carbonic anhydrase. Oxygen-18 exchange catalyzed by an enzyme with rate-contributing proton-transfer steps. Methods Enzymol. **87:** 732–752.

SÜLTEMEYER, D. 1998. Carbonic anhydrase in eukaryotic algae: Characterization, regulation, and possible function during photosynthesis. Can. J. Bot. **76:** 962–972.

———, H. P. FOCK, AND D. T. CANVIN. 1990. Mass spectrometric measurement of intracellular carbonic anhydrase activity in high and low Ci cells of *Chlamydomonas.* Plant Physiol. **94:** 1250–1257.

———, B. KLUGHAMMER, M. R. BADGER, AND G. D. PRICE. 1998. Fast induction of high-affinity HCO_3^- transport in cyanobacteria. Plant Physiol. **116:** 183–192.

TCHERNOV, D., M. HASSIDIM, B. LUZ, A. SUKENIK, L. REINHOLD, AND A. KAPLAN. 1997. Sustained net CO_2 evolution during photosynthesis by marine microorganisms. Curr. Biol. **7:** 723–728.

TORTELL, P. D. 2000. Evolutionary and ecological perspectives on carbon acquisition in phytoplankton. Limnol. Oceanogr. **45:** 744–750.

WOLF-GLADROW, D. A., AND U. RIEBESELL. 1997. Diffusion and reaction in the vicinity of plankton: A refined model for inorganic carbon transport. Mar. Chem. **59:** 17–34.

———, ———, S. BURKHARDT, AND J. BIJMA. 1999. Direct effects of CO_2 concentration on growth and isotopic composition of marine plankton. Tellus **51:** 461–476.

ZONDERVAN, I., R. E. ZEEBE, B. ROST, AND U. RIEBESELL. 2001. Decreasing marine biogenic calcification: A negative feedback on rising atmospheric pCO_2. Glob. Biogeochem. Cycles **15:** 507–516.

Received: 21 June 2002
Amended: 30 August 2002
Accepted: 19 September 2002